Electronic Supplementary Material (ESI) for Journal of Materials Chemistry A.

SUPPLEMENTARY INFORMATION

Insights on Layered Hybrid Solid Electrolyte and Its Application in Long Lifespan High–Voltage All–Solid–State Lithium Battery

Shicheng Yu[a,†,*], Sebastian Schmohl[b,†], Zigeng Liu[a,c,*], Marija Hoffmeyer[b], Nino Schön[a,d], Florian Hausen[a,d], Hermann Tempel[a], Hans Kungl[a], Hans–D. Wiemhöfer[b] and Rüdiger–A. Eichel[a,d]

a. Institut für Energie– und Klimaforschung (IEK–9: Grundlagen der Elektrochemie), Forschungszentrum Jülich, D–52425 Jülich, Germany
b. Institut für Anorganische und Analytische Chemie, Westfälische Wilhelms–Universität Münster, D–48149 Münster, Germany
c. Max–Planck–Institut für Chemische Energiekonversion, D–45470 Mülheim an der Ruhr, Germany
d. Institut für Physikalische Chemie, RWTH Aachen Universität, D–52074 Aachen, Germany

*Corresponding authors: s.yu@fz–juelich.de
zigeng.liu@cec.mpg.de

†These authors contributed equally to this work.

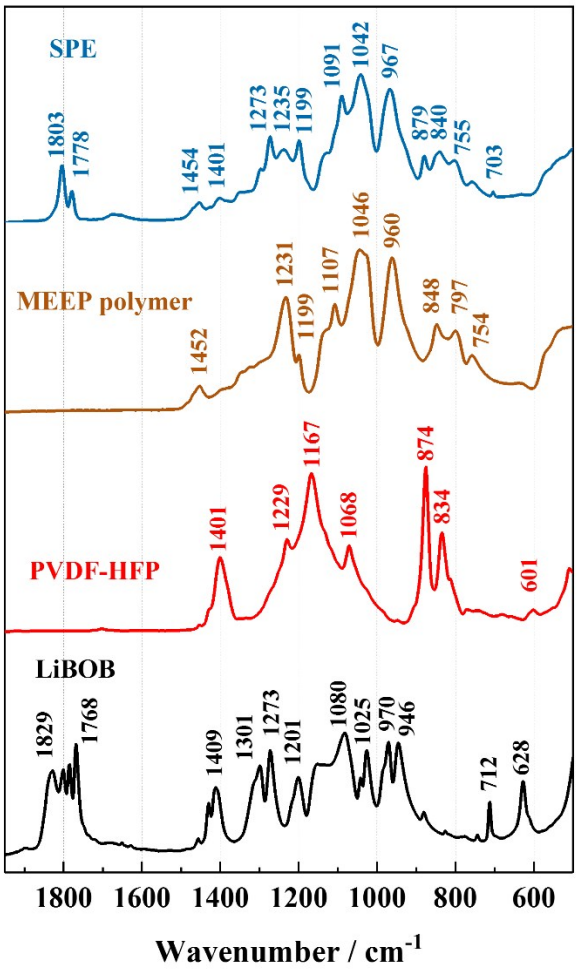

Figure S1 ATR–IR spectra of LiBOB, PVDF–HFP, MEEP polymer and the drop coated solid polymer electrolyte (SPE).

ATR–IR Characterization

Attenuated total reflectance infrared (ATP–IR) spectra were carried out, as depicted in **Figure S1**, for the comparative studies of LiBOB, PVDF–HFP, MEEP polymer and the SPE. The IR spectrum of LiBOB characteristically shows the peaks in the region of 600–720 cm^{-1}, 900–1500 cm^{-1} and 1750–1850 cm^{-1}, corresponding to the COO and B–O_4 deforming frequency, O–B–O and C–O–C asymmetric stretching frequency, the stretching and oscillating frequency of the carbonyl double bond (C=O), respectively. The observed peaks in the range 500–800 cm^{-1} in the PVDF–HFP IR spectrum are corresponding to the α–phase crystals whereas the amorphous β–phase is confirmed by the peaks at 834 and 874 cm^{-1}. Besides, the bands in the region of 1000–1430 cm^{-1} are assigned to the

symmetrical stretching mode and the asymmetrical stretching vibrations of CF_2 group and CH_2 wagging. The IR spectrum of MEEP polymer presents a number of broad peaks in the 750–1500 cm^{-1} region from which the P–N–C, P–O–C, C–O–C, C–N and P=N are found.[S1] The main characteristic peaks of single components are well preserved in the IR spectrum of SPE, as evidence by the fingerprint region between 500 cm^{-1} and 1900 cm^{-1}. Two main regions of interest were identified: (I) the stretching and oscillating frequency of the carbonyl double bond, C=O, observed in the region 1750–1850 cm^{-1} originated from the LiBOB; and (II) the merged and broadened peaks in the range of 700–1460 cm^{-1} were assigned to the representative peaks of the components of LiBOB, PVDF–HFP and MEEP polymer. Comparing the IR spectrum of single components with SPE, the characteristic bands shifted to higher frequencies due to inclusion of salt concentration which confirms the complexation of the electrolyte and the dissociation of LiBOB salt. This indicates only certain amount of salt is able to dissolve that limits the number of generated Li ions.[S2] Moreover, the detected tiny peak for crystalline phase PVDF–HFP appears at 703 cm^{-1} in SPE signifying that a certain level of crystallinity of the polymer electrolyte which improves the mechanical stability. The absence of peaks in the SPE which were observed in the IR spectra of LiBOB, PVDF–HFP and MEEP polymer demonstrating that the two polymers and Li salt are well–mixed without phase separation.

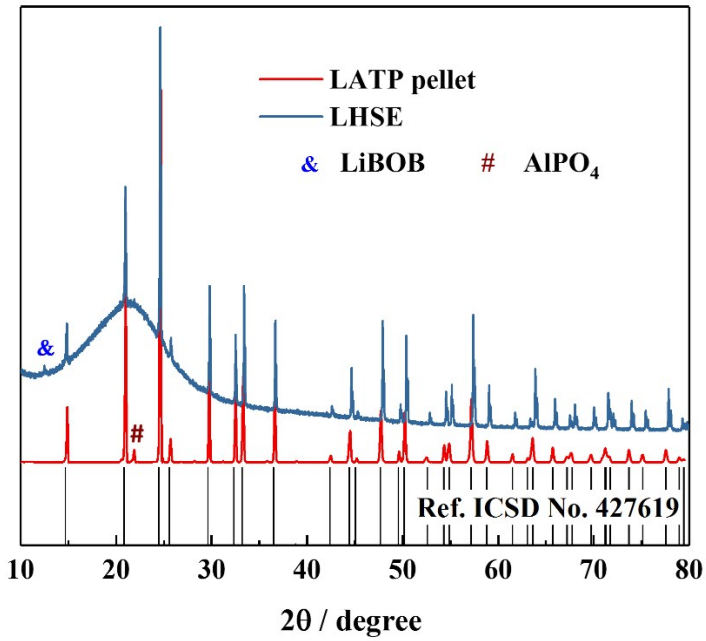

Figure S2 XRD patterns of $Li_{1.3}Al_{0.3}Ti_{1.7}(PO_4)_3$ ceramic pellet and layered hybrid solid electrolyte (LHSE).

XRD Characterization

Phase comparison of the LATP ceramic solid electrolyte and LHSE were evaluated by XRD, as the corresponding diffraction patterns are displayed in **Figure S2**. The LATP pellet can be confirmed with $Li_{1+x}Al_xTi_{2-x}(PO_4)_3$ (space group *R3c*) as main phase and tiny amount of $AlPO_4$ (orthorhombic *C2221* ICSD No. 97546) secondary phase, which was introduced by high temperature sintering process. It has been confirmed that the presence of grain boundary phase, such as $AlPO_4$, could positively affect the ionic conductivity regarding to the improvement of relative density.[S3] The diffraction pattern of LHSE clearly reveals a solid amorphous phase, which corresponds to the MEEP/PVDF–HFP/LiBOB polymer surface layer in this case, whereas the LATP phase is well preserved in the hybrid structure after coating. Moreover, the observed diffraction peak at 13° belongs to LiBOB, suggesting the presence of undissociated Li salt. Comparison of the XRD patterns of the two specimens indicating high chemical stability of LATP with the polymer electrolyte as well as with the solvent used in the drop coating process.

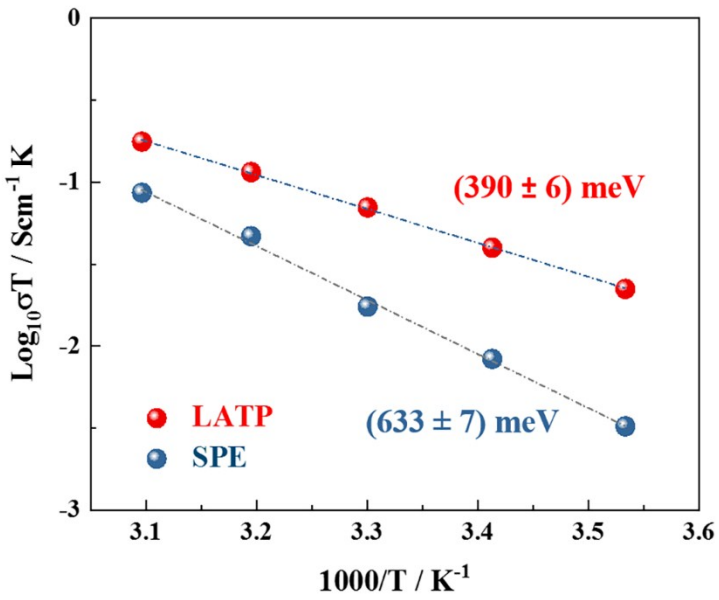

Figure S3 Arrhenius plots of $Li_{1.3}Al_{0.3}Ti_{1.7}(PO_4)_3$ (LATP) and solid polymer electrolyte (SPE) in the temperature range of 10–50 °C. The results are calculated from impedance data measured in the symmetrical cells with Pt electrodes.

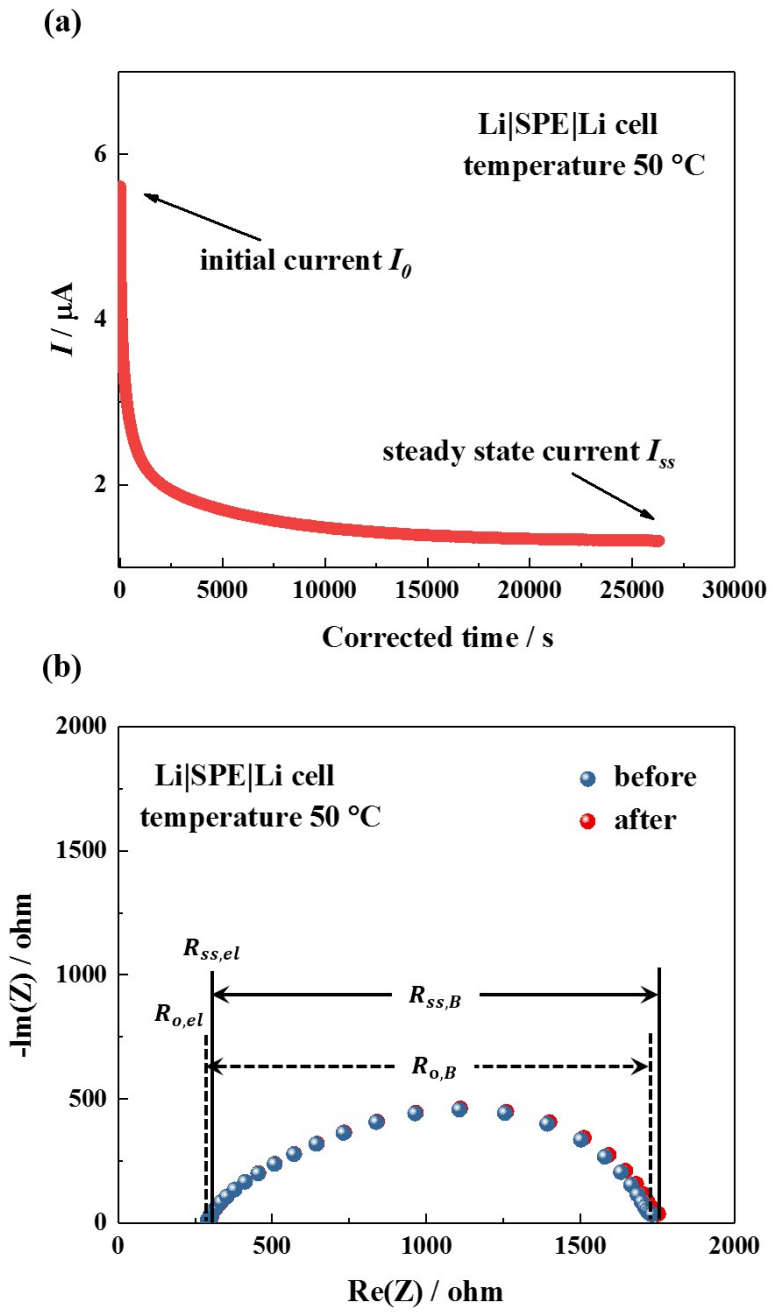

Figure S4 (a) The evolution of current with polarization time under a polarization voltage of 0.01 V and (b) Nyquist plots of the impedance of solid polymer electrolyte (SPE) before and after DC polarization at 50 °C.

Lithium Ion Transference Number of SPE

The lithium ion transference number of SPE is obtained by the combination of chronoamperometry and AC impedance analyses in lithium symmetrical cells, as shown in **Figure S4**. The interface impedance was measured at the beginning and at the end of the

polarization in order to determine correction factors which eliminate the influence due to any small drifts of the interface resistances. The ohmic part of the metal/polymer interface impedance, namely the resistances $R_{0,B}$ (before polarization) and $R_{SS,B}$ (steady state) were determined by analyzing the frequency dependent impedance in the range of 100 kHz to 1 Hz. They were used to eliminate the SEI contribution in the final evaluation from the bulk polarization voltage.[S4, S5] After switching-on the DC voltage, the time dependent current I_t was monitored. The initial current (I_0) and the final steady-state current (I_{ss}) were taken for the calculation of the transference number t_+ according to

$$t_+ = \frac{I_{SS}(\Delta V - I_0 R_{0,B})}{I_0(\Delta V - I_{SS} R_{SS,B})} \qquad (1)$$

In order to take into account the change of the electrolyte resistance from $R_{el,0}$, to $R_{el,ss}$ during DC polarization that caused by the formation of a concentration gradient, an additional correction according to Abraham et al.[S5] was introduced. This correction leads to the following final equation and was used in our experiments:

$$t_+ = \frac{I_{SS} R_{el,ss}(\Delta V - I_0 R_{0,B})}{I_0 R_{el,0}(\Delta V - I_{SS} R_{SS,B})} \qquad (2)$$

As demonstrated in **Figure S4**, while increasing the polarization time, the current reaches the steady state. The obtained Li^+ transference number $t_{+,SPE}$ at 50 °C for SPE is 0.06. The low lithium ion transference number value is attributed to the molecular structure of MEEP that cause of the strong lithium coordination between the oligoether sidechains and the nitrogen atom inside polyphosphazene backbone.[S6]

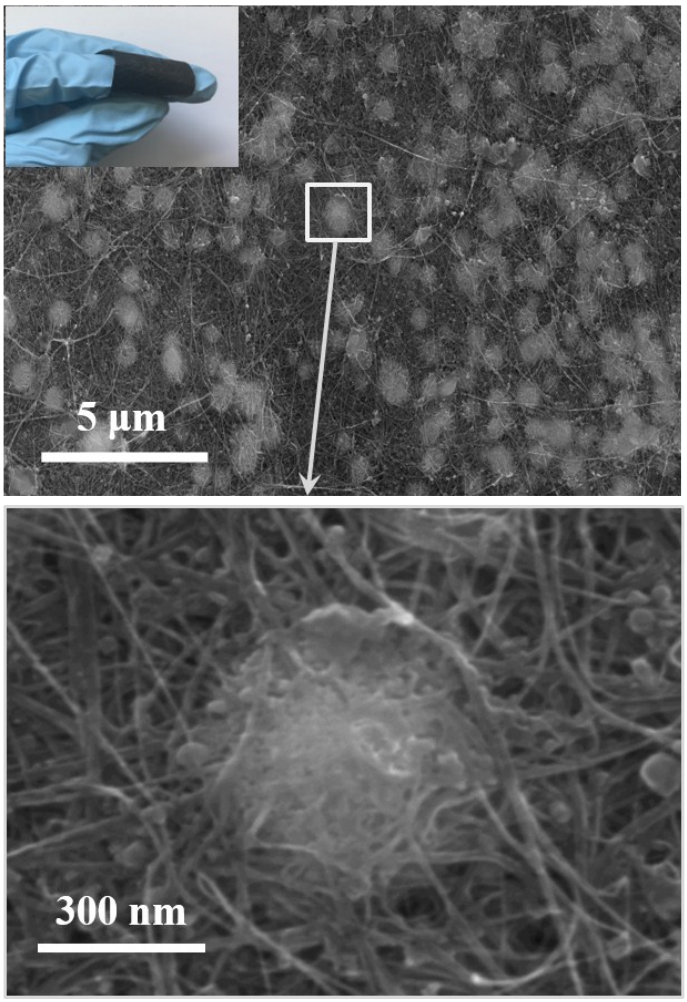

Figure S5 SEM images of the binder–free, current collector–free, flexible carbon nanotube enhanced $Li_3V_2(PO_4)_3$ cathode.

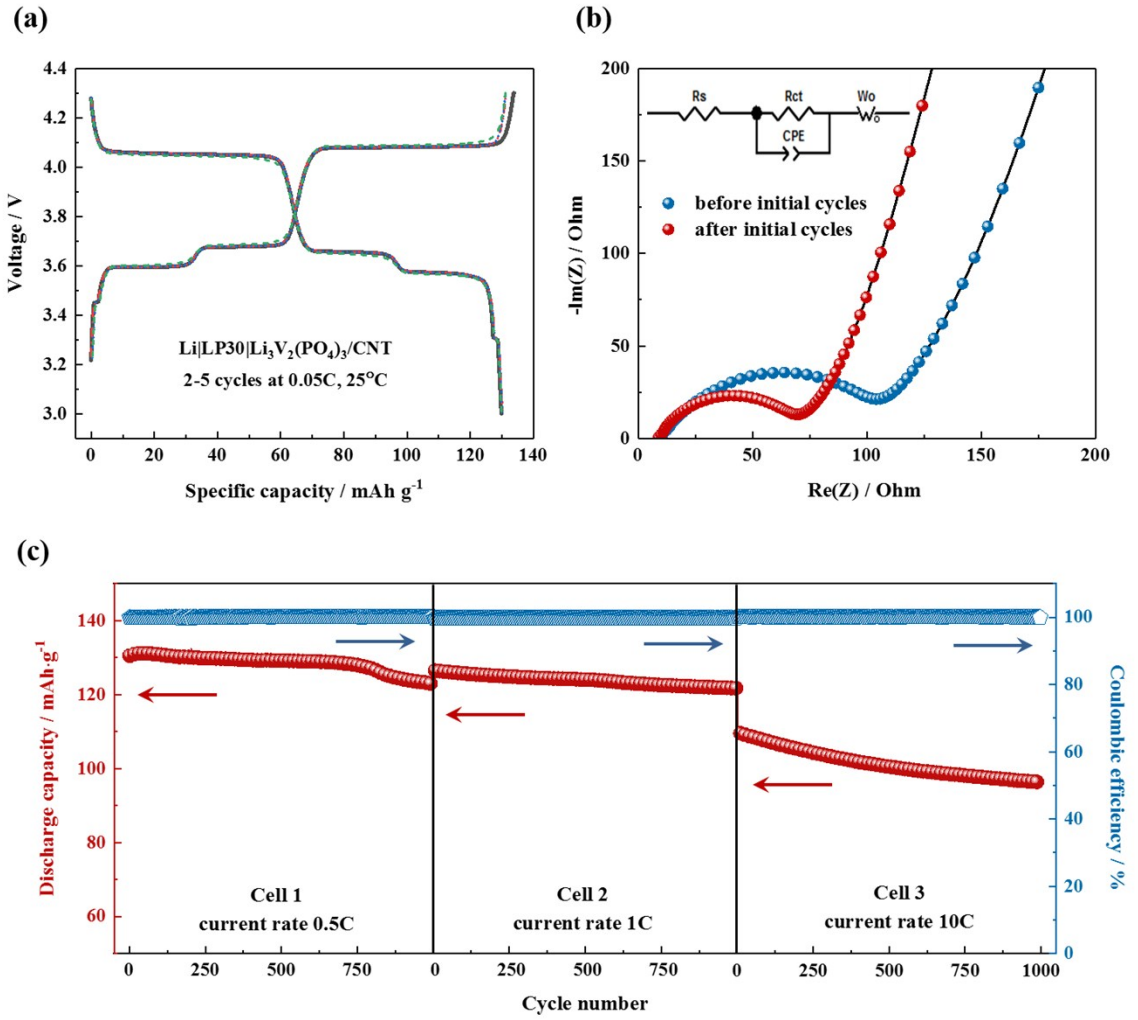

Figure S6 Electrochemical performances of cells with lithium anode, $Li_3V_2(PO_4)_3$/CNT cathode and liquid electrolyte of LP30 (1M $LiPF_6$ in EC : DMC (1:1 vol.%)). (a) Initial charge–discharge profiles of formation cycles, (b) impedance before and after formation cycles, and (c) cycling performance at 0.5C, 1C and 10C respectively. All the electrochemical measurements were performed at 25 °C.

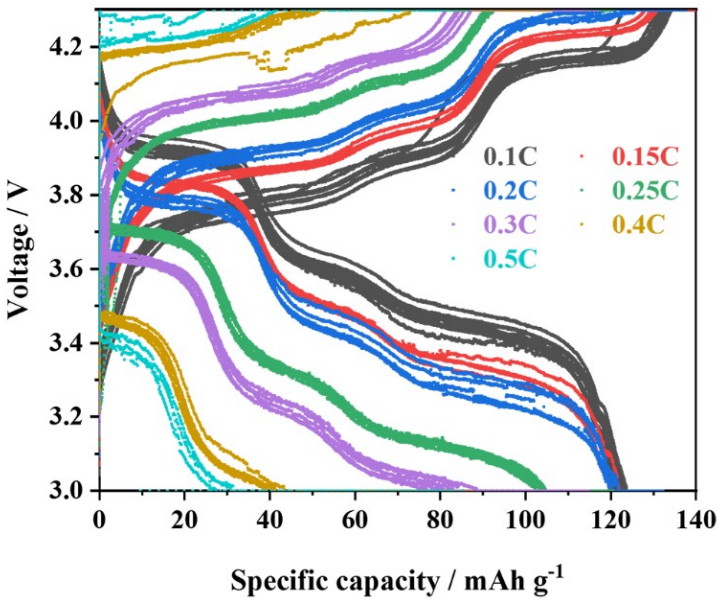

Figure S7 Charge–discharge curves of Li|layered hybrid solid electrolyte|$Li_3V_2(PO_4)_3$/CNT all–solid–state lithium battery at current rates of 0.1C, 0.15C, 0.2C, 0.25C, 0.3C, 0.4C and 0.5C for five cycles, respectively, at 50 °C.

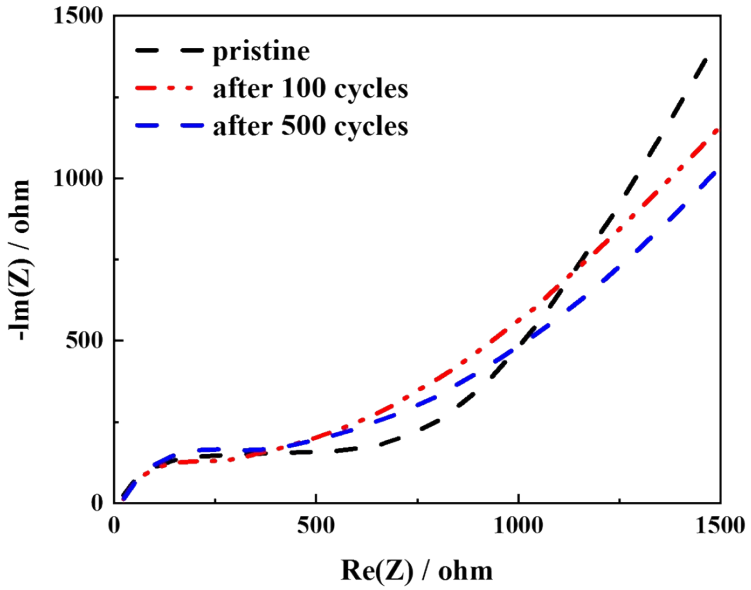

Figure S8 Nyquist plots of Li|layered hybrid solid electrolyte|$Li_3V_2(PO_4)_3$/CNT all–solid–state lithium battery at pristine state, after 100 cycles and after 500 cycles at 0.2C at 50 °C.

EIS During Long-Term Cycling

The impedance measurement was performed on the battery at the pristine state, after 100 cycles and after 500 cycles, respectively. The overall battery resistance slightly decreased after the first hundred cycles and kept basically constant until the end of long-term cycling, indicating a high electrochemical stability of the prepared battery. However, since the processes are highly overlapped in the frequency range, further analyses are ongoing in order to resolve the results.

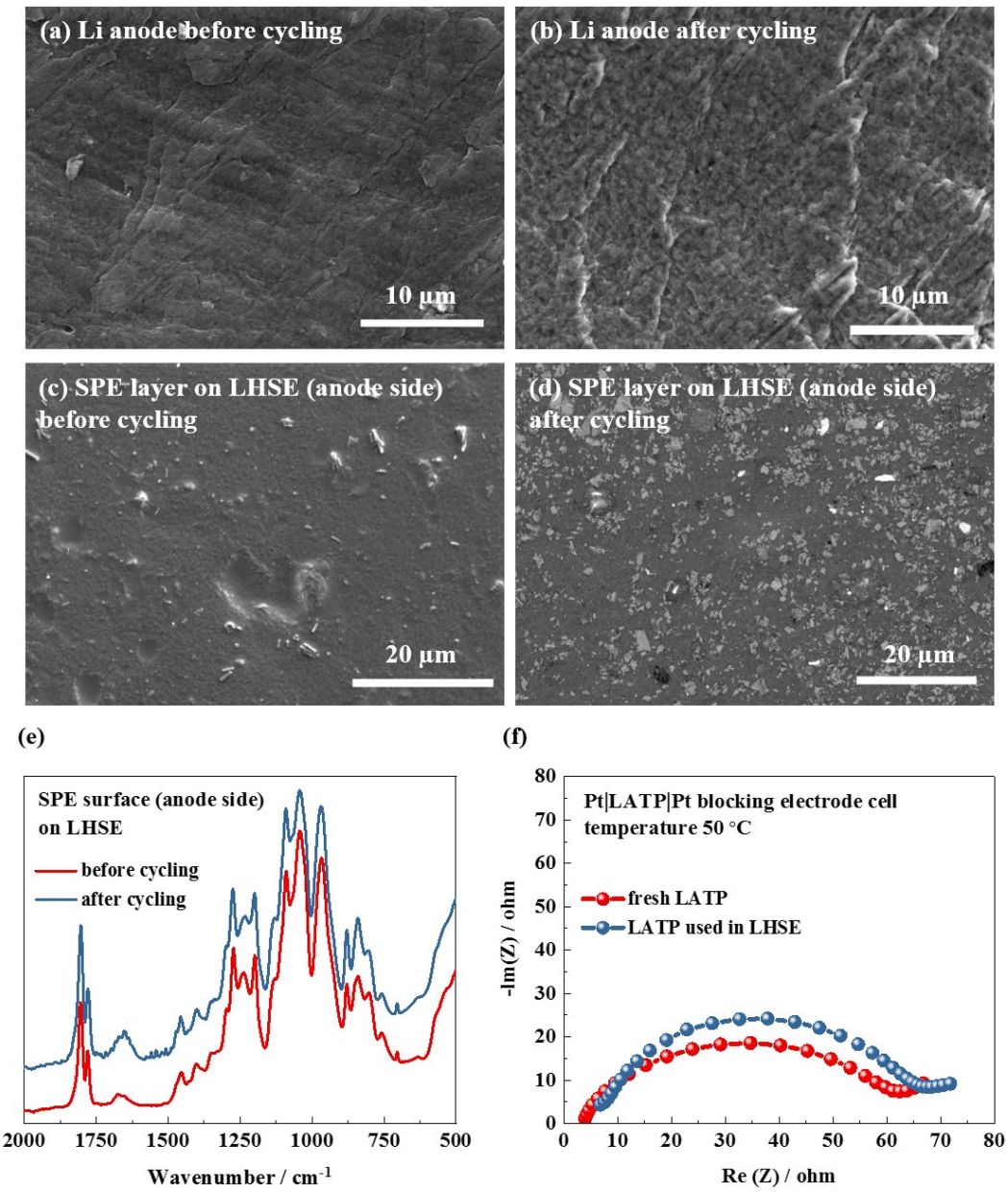

Figure S9 Surface SEM images of lithium anode ((a) and (b)) and solid polymer electrolyte (SPE) ((b) and (c)) on the layered hybrid solid electrolyte (LHSE) before and after 500 cycles at 50 °C. (e) ATR–IR spectra of the SPE surface before and after 500 cycles. (b) Nyquist plots of the fresh LATP and the LATP used in LHSE after 500 cycles.

Post–Test Characterization

To shed light on the stability and compatibility of the LHSE with metallic lithium anode, SEM characterization on the lithium anode and the SPE, which was in direct contact with lithium metal, is performed after the disassembly of the Li|LHSE|$Li_3V_2(PO_4)_3$/CNT

battery which finished long–term cycling. The surface region on both samples were marked before cycling to gain relative comparison. As can be seen in the SEM images in **Figure S9**(a) and (b), after cycling, the roughness of lithium surface is increased but no cracks and dendrites were observed on the surface of lithium, which can be attributed to a relatively uniform Li^+ flux across the interface between Li and SPE. Except some lithium was left on the surface of SPE, as shown in **Figure S9**(c) and (d), the morphology of SPE become smoother after long term cycling, owing to the constant pressure on the soft polymer layer between lithium metal and LATP pellet. The chemical composition of SPE, after contacting with lithium metal for a long time cycling, is checked by ATR–IR spectra, where all the characteristic peaks are well preserved, as shown in **Figure S9**(e), indicating high electrochemical compatibility of SPE with lithium in the relevant potential range of 3.0–4.3 V. The electrochemical compatibility of the LATP, which was used in the long–term cycled all–solid–state battery, is studied by comparing the impedance measurement in a Pt|LATP|Pt blocking electrode cell at 50 °C, as presented in **Figure S9**(f). The charge transfer resistance of the LATP after cycling is slightly increased, while the total ionic conductivity decreased from 0.45 to 0.42 mS cm^{-1}, meaning the success in the integration of LATP with metallic lithium anode, with the help of SPE, in the all–solid–state batteries.

References

[S1] Y. W. Chen-Yang, J. J. Hwang and A. Y. Huang, *Macromolecules*, 2000, **33**, 1237–1244.

[S2] S. A. M. Noor, A. Ahmad, I. A. Talib and M. Y. A. Rahman, *Ionics*, 2010, **16**, 161–170.

[S3] S. Yu, A. Mertens, X. Gao, D. C. Gunduz, R. Schierholz, S. Benning, F. Hausen, J. Mertens, H. Kungl, H. Tempel and R.-A. Eichel, *Funct. Mater. Lett.*, 2016, **09**, 1650066.

[S4] M. M. Hiller, M. Joost, H. J. Gores, S. Passerini and H. D. Wiemhöfer, *Electrochim. Acta*, 2013, **114**, 21–29.

[S5] K. M. Abraham, Z. Jiang and B. Carroll, *Chem. Mater.*, 1997, **9**, 1978–1988.

[S6] S. Jankowsky, M. M. Hiller and H. D. Wiemhöfer, *J. Power Sources*, 2014, **253**, 256–262.